2022

Demonstration of Thermal Energy Storage System with Salt Hydrate Phase Change Material Composite

Jason Robert Hirschey

Kyle R. Gluesenkamp

Samuel Graham

Demonstration of Thermal Energy Storage System with Salt Hydrate Phase Change Material Composite

Jason Hirschey[1]*, Kyle R. Gluesenkamp[2], Samuel Graham[1]
[1]George W. Woodruff School of Mechanical Engineering, Georgia Institute of Technology
North Ave NW, Atlanta, GA, USA
jhirschey13@gatech.edu

[2]Oak Ridge National Laboratory
1 Bethel Valley Rd, Oak Ridge, TN, USA

* Corresponding Author (jhirschey13@gatech.edu)

ABSTRACT

Thermal energy storage (TES) decouples heat generation from use, providing a crucial tool to mitigate fluctuating thermal loads. TES systems may often contain a phase change material (PCM) which stores heat isothermally through the enthalpy of phase change, and thus the TES as a whole operates at a near constant temperature. Integrated into a heat pump (HP) or heat transfer fluid (HTF) circulation loop, the TES will behave as an isothermal heat exchanger (HX), absorbing or releasing heat into the HTF. For near-ambient TES (-15-85°C), solid-liquid PCMs provide the highest energy storage density. However, the PCMs available in this temperature range often have low thermal conductivity that hinder the power capacity of a TES. As such, modifications such as metallic extended surfaces or fins are made to the TES to increase its power capacity. This work instead uses an enhanced PCM composite material in a simple and scalable shell-and-tube design. In this work, two prototype-scale TES units are demonstrated: 1) a benchtop scale unit as a proof-of-concept with targeted specifications 50 W, 100 Wh, and 2) an intermediate scale with target specifications 200 W, 0.8 kWh. The PCM composite is based on sodium sulfate decahydrate (SSD) and high thermal conductivity expanded graphite (EG). Both TES units containing this material met or exceeded design performance. The design, production method, and performance results are discussed.

Keywords: *Thermal energy storage, heat exchanger, salt hydrate, graphite, phase change material*

1. INTRODUCTION

Thermal energy storage (TES) is a powerful energy storage mechanism that is perfectly suited for applications where the end use is heat. TES may be especially useful for low-grade thermal energy near ambient temperatures which traditionally rely on a near-instantaneous conversion of one energy form into heat. For example, heat pumps and refrigeration cycles typically utilize electrical energy to move thermal energy for heating or cooling the target application, or resistive heating elements that convert electrical energy or furnaces that convert chemical energy into thermal energy for heating applications. TES provides a tool that may enable an application to decouple this conversion, and also may offer a solution for capturing and reusing waste heat.

Two important characteristics of any TES system are the quantity of heat storable within, and the rate at which this heat can be dispatched or moved in and out of the TES. The energy storage capacity of a TES is almost entirely dictated by the materials used. Including a phase change material (PCM) into the TES sharply increases its energy storage capacity; through the latent heat of phase change, the PCM can isothermally absorb and release quantities of heat much greater than most sensible thermal storage. Furthermore, the PCM allows the TES to operate nearly isothermally, a feature which can improve reliability and target TES for specific applications.

The thermal power of a TES is dictated by the materials and application, but also largely dependent on the geometry of the system. Material thermal conductivity and thermal effusivity characterize the ability of these materials to move heat through themselves. But heat moving in and out of the TES relies on its geometric interfacing with external heat transfer surfaces. In this sense, a TES system may be considered an isothermal heat exchanger (HX) that couples in some way to its application. The TES could be integrated into a heat pump (HP) refrigeration loop or some other heat transfer fluid (HTF) circulation loop. Often, extended metallic fins or complex serpentine coils are used to increase the heat transfer contact area thereby increases TES thermal power (Abdulateef *et al.*, 2019; Asgari *et al.*, 2021; Herbinger & Groulx, 2022; Pakalka *et al.*, 2020). However, these features displace PCM lowering the energy storage capacity and may not be cost-effective at large scales. To this end, this work presents a TES PCM-HX design with a PCM composite material of enhanced thermal conductivity and a simple HX design to demonstrate that high TES thermal performance can be achieved in a scalable design.

In this work, the design and performance of two TES units are presented. The two TES discussed are 1) a small benchtop unit with target specifications nominally 50W of thermal power and 100Wh of thermal energy, called TES-α, and 2) a larger unit with target specifications nominally 200W of thermal power and 800Wh of thermal energy, called TES-β. The PCM is a composite salt hydrate and expanded graphite. The addition of the graphite increases the bulk thermal conductivity of the PCM, negating the need for fins or extended heat exchanger surfaces in the HX. This work evaluates the viability of this design and PCM-graphite composites materials for TES systems.

2. MATERIALS

The TES are based on a shell-and-tube design. The shell is sourced from standard schedule 40 PVC pipe, and the tube is standard ¼ in. outer diameter copper pipe. PVC knockout caps are used to encapsulate the PCM in the shells. The caps are epoxied to the shells using a two-part steel enforced epoxy.

The PCM is a composite of consisting of mainly salt hydrate and graphite. The salt hydrate is sodium sulfate decahydrate, $Na_2SO_4 \cdot 10H_2O$, (SSD). The salt was sourced in its anhydrous form from Alfa Aesar. The graphite is expanded graphite (EG) which has been commonly studied for use in PCM composites (Fang *et al.*, 2019; Mao *et al.*, 2017; Ye *et al.*, 2017). The SSD, EG, and other materials are mixed and compressed into the annulus of the HX shells.

For TES-α, borax, $B_4O_7Na_2 \cdot 10H_2O$, was added as a nucleating agent and sodium polyacrylate (SPA) added as a thickening agent. Borax is historically a nucleating agent for SSD due to similar crystal characteristics (Ruben *et al.*, 1961; Telkes, 1952). The borax and SPA were sourced from Alfa Aesar. For TES-β, borax was again added as a nucleating agent. Dextran sodium sulfate (DSS) was added as a thickening agent. Both sourced from Alfa Aesar. The change in thickening agent is a result of research conducted between the fabrication and testing of the two TES units analyzed here; the DSS showed greater stability in repeated thermal cycling tests (Li *et al.*, 2022).

The composition of the PCM composites of both TES units are reported by mass percent in Figure 1. Both units were composed of several individual modules that were assembled containing PCM in these same ratios, although some variations exist between modules for each. The total PCM composite mass for TES-α was 3.2 kg with a packing density of 0.84 kg/m^3. The total PCM composite mass for TES-β was 27.537 kg with a packing density of 0.92 kg/m^3. The additional material and their ratios relative to the SSD were not arbitrary; they were found to be high performing material compositions based on other research being conducted congruently to this work. The details of why these materials are chosen and in what ratios are outside the scope of this present work.

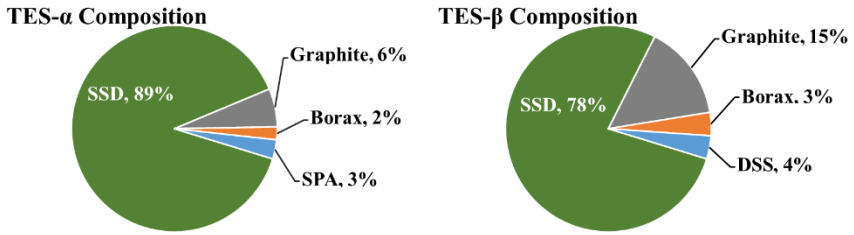

Figure 1. PCM composite composition for the two TES in mass percent

3. DESIGN

The design of these TES units is a pseudo shell-and-tube design. Figures 2 & 3 depict the general geometry of these two designs. The HTF passes through an axially centered copper tube; the total metallic content composes less than 5% of the total TES volume. The PCM is packed into the annulus of the shell. The shell is PVC plastic material which is low thermal conductivity and acts as a relative insulator. The TES modules are wrapped in insulating foam during testing. Thermocouples are placed in the HTF stream at the inlet and outlet of all modules. A mass flow meter measures the HTF flow rate.

The dimensions of each design were determined by an iterative process. With certain target performance metrics (power, energy, time), known PCM composite and HTF thermophysical properties (phase change temperature, enthalpy, density, specific heat), and capabilities and standard dimensions of the instrumentation available (pump flow rate, hot water and cold water bath temperature limits, standard copper tubing dimensions, stand PVC dimensions), a series of equations were found to relate these constraints to the unknown quantities: overall TES length, number of parallel TES modules, inlet and outlet target temperatures, and desired flowrate.

Figure 2 illustrates the iterative design process to achieve the defined TES performance metrics. There are two classes of design variables: selectable and customizable. Selectable variables include standard sized, off-the-shelf components: schedule 40 PVC shell size, copper tube size, PCM properties. Customizable variables include parts that are easily adjusted around the selectable variables, such as HTF flow rate and temperature, and number of modules in parallel or series. The first step in the iterative design process is arbitrarily choosing some selectable variables. Then the customizable variables are tuned to meet certain criteria for the TES, including the performance metrics, but also more tangible metrics like size and weight, and some less tangible metrics like if the design can be produced in the lab with the tools available. A series of equations were written containing heat transfer, thermodynamic, and fluid dynamics relationships to check for consistency in power and energy between the HTF and the TES. These relationships capture most of the selectable and customizable variables, and most are reversible so that the process could be done if other metrics are important considerations, if necessary.

As an example of the design process, the thermal energy performance metric is used to determine the quantity of PCM composite necessary in the annulus of the shell-and-tube design based on the phase change enthalpy and density of the PCM composite. Once the diameter of schedule 40 PVC shell and copper tube size are selected, the quantity of necessary PCM informs the overall length of the TES. This length influences the necessary HTF flow rate, and inlet and outlet temperatures to achieve the desired thermal power metric. Fluid dynamics equations would be used to compute the HTF heat transfer rate, and this compared to heat transfer equations on the PCM composite under these temperature conditions to ensure thermodynamic consistency. On the last step, the feasibility of production was considered for the determined size of each TES module. If infeasible, one selectable variable would be changed and the process repeated until a feasible design met all considerations.

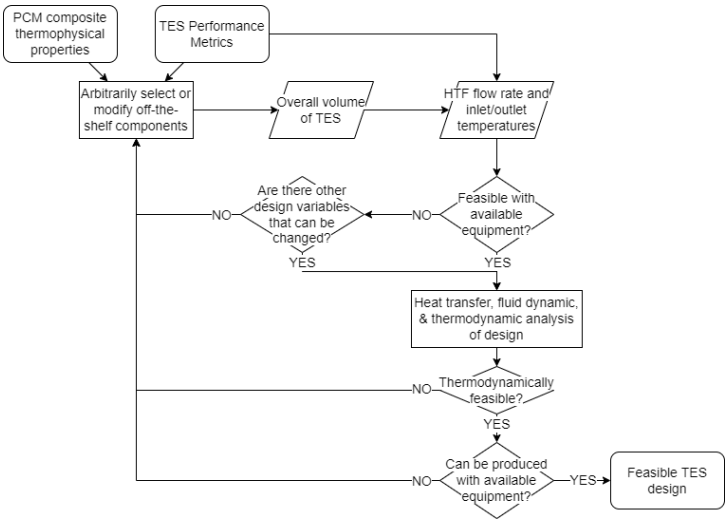

Figure 2. TES iterative design process overview

For each TES system, the PCM composite material was synthesized in large quantities. The graphite-PCM material was then compressed into the annulus of the shell-and-tube design with the tube in place, shown in Figure 3: A) The material was first poured into the shell (A) until nearly full (B). A piston/plunger added atop the material (C). Handheld bar clamps used to apply even force, compressing the material (D). Several piston/plungers of varying sizes were used to compress deep into the shell. Processes A-D repeated until the shell is filled before being capped (E). This process resulted in good thermal contact between the tube and the PCM composite material. Producing several identical modules increases the scalability of this design; several modules may be attached to achieve certain performance metrics by following the process outlined in Figure 2.

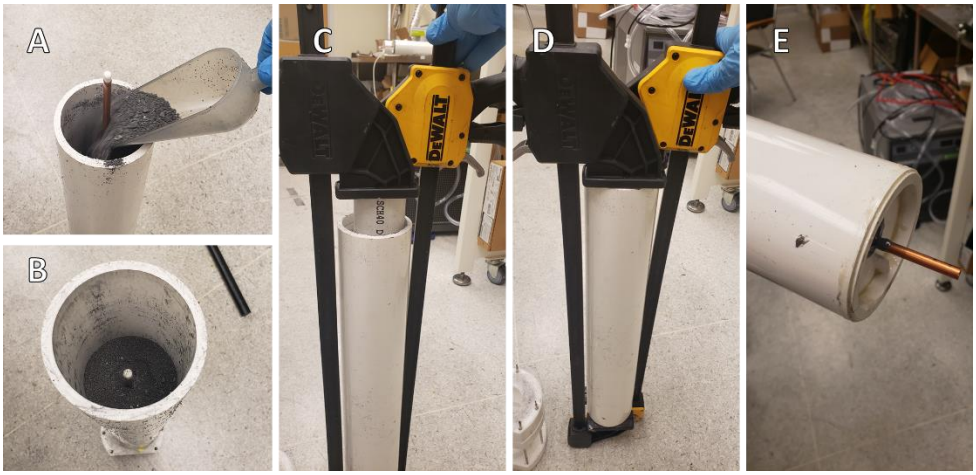

Figure 3. Process of compressing PCM composite into TES shell

For TES-α, two shell-and-tube modules were synthesized. These were arranged in series with each other. Figure 4 shows the dimensions of this design and the design installed on the test bed before insulation foam was added to the exterior of the shells. A peristaltic pump was needed to throttle the HTF flow rate from the hot water bath and the chillder for this small TES size.

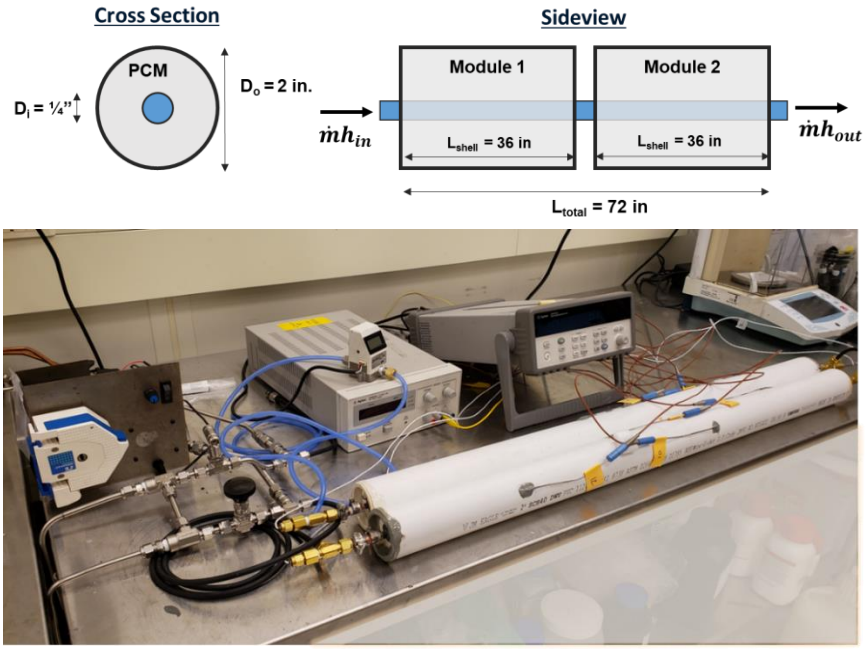

Figure 4. TES-α dimensions and test bed setup

For TES-β, fourteen shell-and-tube modules were constructed. They were arranged in two banks in series composed each of seven modules in parallel. Figure 5 shows this arrangement and the TES on the testbed with insulating foam blanketing the two banks.

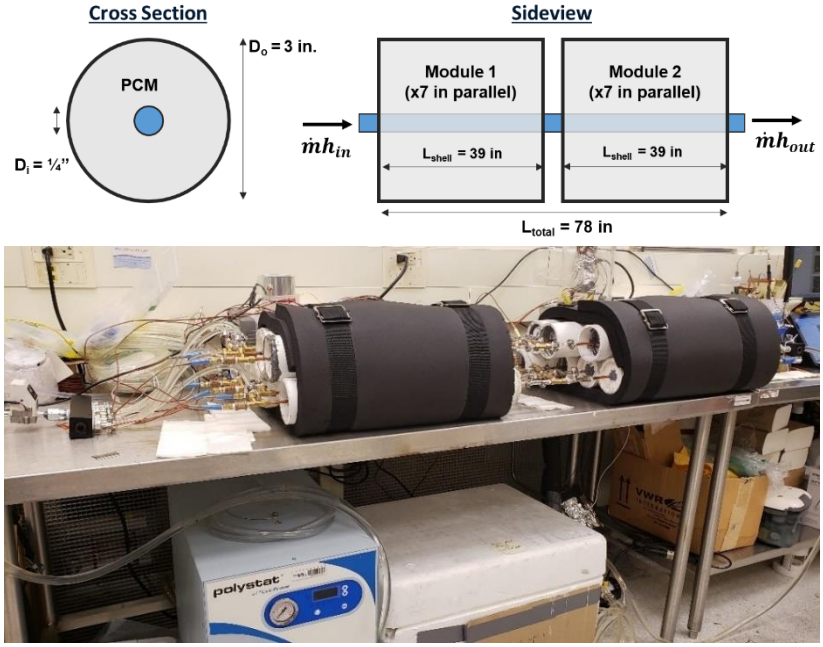

Figure 5. TES-β dimensions and test bed setup

4. OPERATION & POWER CALCULATION

The HTF used in these TES units is water which has well-characterized thermophysical properties for ease in analysis. Two water baths, one hot and one cold, are separately controlled with PID temperature controls. The cold bath is a Cole-Parmer Polystat chiller with integrated water pump. The hot bath is a custom-built system with an external water pump and enclosed in an insulating chamber. Details of this hot water bath are omitted for brevity; any commercially available or custom-built water bath capable of maintaining a constant temperature and pumping water with steady flow rate will suffice in replicating this experiment.

The baths are connected to the TES units with three-way valves that enable the operator to switch between heating and cooling modes. Figure 4 depicts the orientation of the water baths on TES-β.

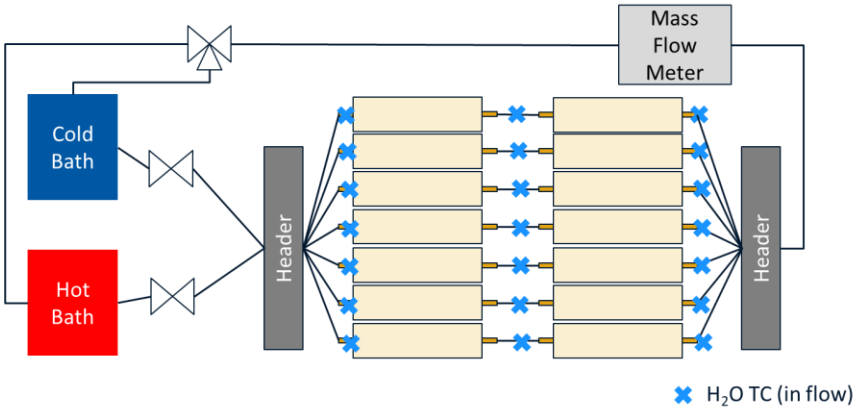

Figure 4. Integration of TES-β with hot- and cold-water baths

Thermocouples are embedded in the HTF stream, and the thermocouple measurement location are placed approximately at the inlet and outlet of each TES module. For TES-β, a header splits the flow into the seven parallel shells. It is assumed that the flow is split approximately evenly between the seven parallel pathways.

The calculation of thermal power *P(t)* is done by measuring the HTF temperature difference at the inlet and the outlet of the TES modules multiplied by the mass flow rate, $\dot{m}(t)$, and the specific heat of the HTF, $c_{p,HTF}$, Eq. 1. However, the HTF takes some time to traverse from the inlet to the outlet. Thus, rather than measuring an instantaneous spatial HTF temperature difference, Eq. 1 is modified to measure a temporal HTF temperature difference. This is accomplished by offsetting the time reading of inlet temperature by τ which is the calculated time the water travels from inlet to outlet. τ is calculated by using the flow rate measurement, density of the HTF, and geometry of the tube in the TES unit.

$$P(t) = \dot{m}(t) * c_{p,HTF} * (T_{HX,in}(t-\tau) - T_{HX,out}(t)) \quad (1)$$

The total energy *E(t)* is determined by integrating the power over time of operation, Eq. 2.

$$E(t) = \int_{t=0}^{t=end} P(t)\, dt \quad (2)$$

5. RESULTS

The thermal power and energy results of TES-α are shown in Figures 5 & 6 for a single heating cycle. The green region of Figure 5 shows a time of approximately 1 hour wherein TES-α maintained a thermal power greater than the target of 50W. This small TES required the peristaltic pump to be adjusted mid-experiment which explains the jumps in the power curve prior to this window and at the end of the experimental run. Note how the first shell in series is responsible for nearly twice as much power as the second shell during the first three hours of the run, then its performance drops below the second shell drastically. This is the effect of phase change within the TES-α. Once the phase change is complete on the first shell, it is incapable of storing heat isothermally and thus its temperature rises to match the HTF, significantly reducing the driving temperature and lowering its effect on overall thermal power. Real systems utilizing this design will need to account for this drop in power.

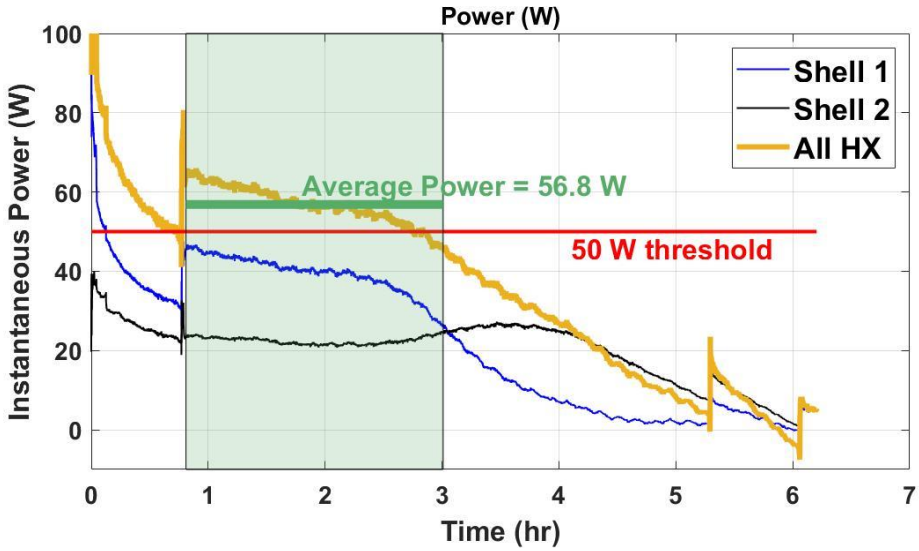

Figure 5. Thermal power of TES-α

Figure 6 shows the cumulative energy stored within the TES-α during this same heating cycle. The target for this TES-α was 100 Wh of storage which was exceeded by ~20% in the green highlighted window, within added the factor of safety. Even if some energy stored is accounted for by sensible storage, the majority is assumed to be latent storage of the PCM due to the plateaued power curve of Figure 5.

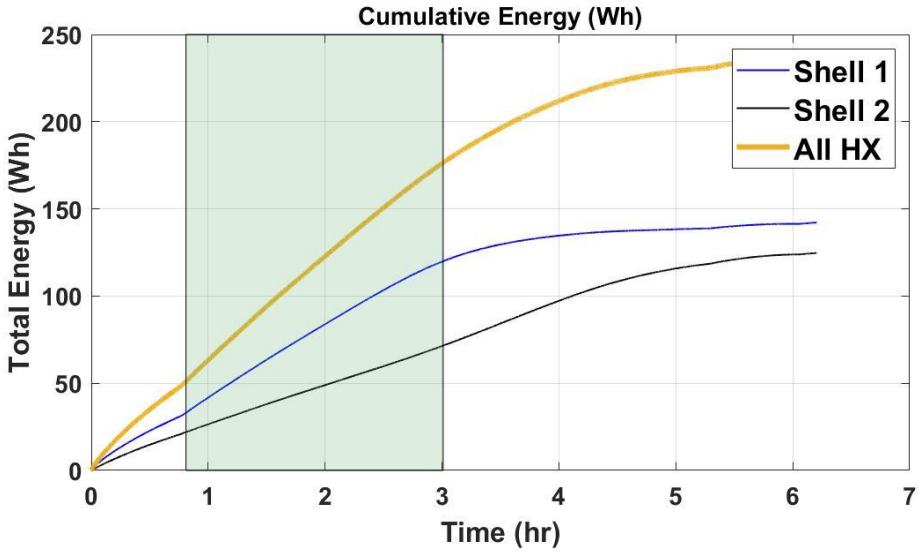

Figure 6. Thermal energy storage of TES-α

The thermal power results of TES-β are shown in Figure 7. A large spike of thermal power at the beginning of the test is due to sensible heating from the relatively cold steady state to the sudden influx of relatively hot HTF. However, once the power settles from this initial spike, its output is nearly 2-3 times the expected value. It was later understood that the HTF flow rate and the hot water bath temperature were both higher than was planned, an oversight by the operator. As such, the power for each bank in this TES achieves > 200 W of thermal power for nearly two hours.

Due to the flowrate mishap, there is no clear distinction between the first and second bank of tubes like was observed between the first and second modules in TES-α. It is speculated that the higher-than-expected flow rate moved the HTF though the TES more quickly than the initial design calculations predicted. As such, the HTF temperature change was small for each bank of the TES and thus each bank saw approximately the same thermal forcing temperature gradient. Paired with slight variations in the 14 TES modules, both the first and second bank acted approximately identically. In a real system, this may be ideal; there may not be a performance drop until all TES capacity is depleted. But this is erroneously done here.

After operation for 2 hours, the hot water bath water pump developed a leak. An attempt to patch the leak mid-test was unsuccessful and the test had to be aborted after 2.5 hours.

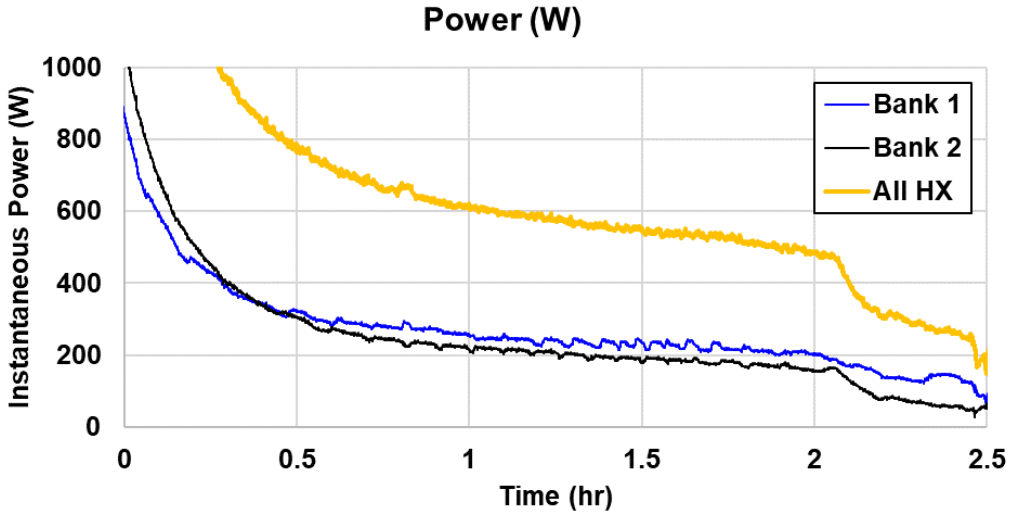

Figure 7. Thermal power of TES-β

Despite the issues encountered during the testing of TES-β, its energy storage far exceeded the performance metric, as shown by Figure 8. Even if the initial spike at the start of the test is ignored, and the period between 0.5 and 2.5 hours is analyzed, this TES stored over 1 kWh of thermal energy. This higher-than-designed energy storage is not surprising as the updated PCM composite mixture was seen to have much higher performance than the PCM composite mixture in TES-α, with higher enthalpy and more stability, but this was not updated in the TES design process. The energy storage values are reasonable and within the designed factor of safety once accounting for the updated thermophysical properties. However, because the test was aborted early, the heat leakage rate was unable to be quantified. As such, some of this energy may be lost to the ambient and not truly stored in the TES.

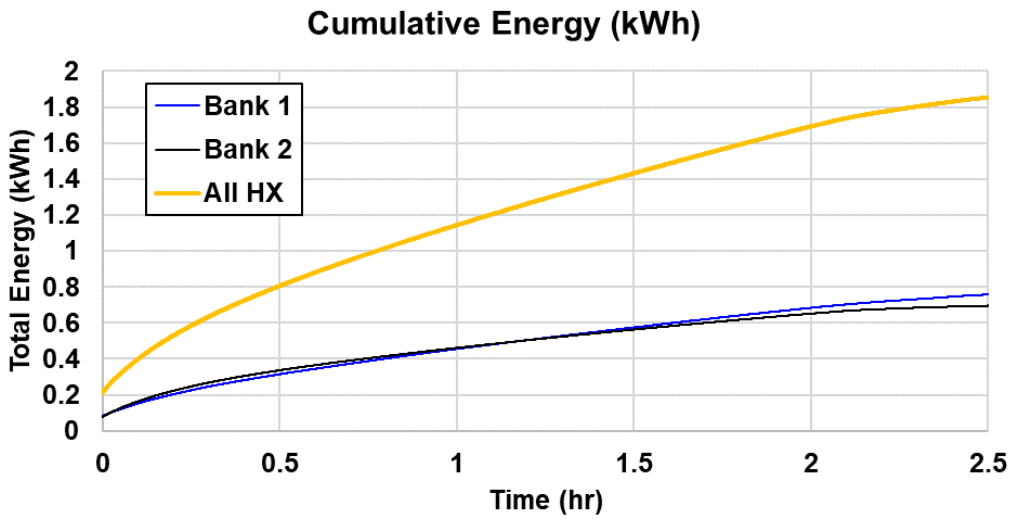

Figure 8. Thermal energy storage of TES-β

Furthermore, this TES-β showed that the design was capable of high thermal power performance. This exemplifies the potential for TES systems containing an enhanced PCM-graphite composite material in a simple and scalable shell-and-tube HX setup; no extended metallic fins, heat exchange surfaces, or complex designs were necessary to achieve high performance.

6. CONCLUSION

Thermal energy storage (TES) is an ideal mechanism for recouping waste heat that may be used in applications where low-grade heat is the end use: refrigeration, indoor heating and cooling, domestic hot water. TES system are often characterized by its energy storage capacity and its thermal power which will vary between applications.

Implementing a phase change material (PCM) into TES can drastically improve the energy storage capacity by leveraging the latent heat of phase change as an isothermal heat source or sink. In regard to increasing the thermal power, the TES with integrated PCM may be better described as a PCM heat exchanger (HX). These PCM HX have been the subject of much research, but typically rely on some metallic extended finned surface or complex geometry to aid in moving heat in and out of the TES and to the target application.

This work demonstrated a high performing TES using a simple shell-and-tube geometry and an enhanced high thermal conductivity PCM composite material made of an inorganic salt hydrate and expanded graphite. Two TES units were demonstrated: a 50W, 100Wh proof-of-concept (TES-α), and a 200W, 800Wh intermediary to a full-scale TES system (TES-β). The design was based on an iterative method that factored in the constraints of the equipment available, commercially available products, and a laboratory-based manufacturing process without heavy equipment.

TES-α performed as designed, averaging 56.8W of thermal power for 1.2 hours, and ~120Wh of thermal energy in this time. TES-β encountered issues during test, but still surpassed the target performance metrics. This system

experienced over 400W of thermal power for over 1.5 hours and stored over 1kWh of thermal energy. The success of the TES-β is attributed to adjustments to the experimental test bed as a result of lessons learned from the TES-α, and an improved PCM composite recipe with higher enthalpy and more stability.

These tests show that high performing, high thermal conductivity PCM composite materials can be effectively utilized in simple TES system geometries without the need for extended heat transfer surfaces. Future work will explore these TES designs for stability, adjustable power modes, and heat pump integration.

NOMENCLATURE

TES	Thermal Energy Storage
PCM	Phase Change Material
HP	Heat Pump
HTF	Heat Transfer Fluid
HX	Heat Exchanger
TES-α	Benchtop demonstration unit with targeted specifications 50 W, 100 Wh
TES-β	Larger demonstration unit with targeted specifications 200 W, 0.8 kWh

REFERNCES

Abdulateef, A. M., Abdulateef, J., Sopian, K., Mat, S., & Ibrahim, A. (2019). Optimal fin parameters used for enhancing the melting and solidification of phase-change material in a heat exchanger unite. *Case Studies in Thermal Engineering*, 100487. doi:https://doi.org/10.1016/j.csite.2019.100487

Asgari, M., Javidan, M., Nozari, M., Asgari, A., & Ganji, D. D. (2021). Simulation of solidification process of phase change materials in a heat exchanger using branch-shaped fins. *Case Studies in Thermal Engineering, 25*, 100835. doi:https://doi.org/10.1016/j.csite.2020.100835

Fang, Y., Ding, Y., Tang, Y., Liang, X., Jin, C., Wang, S., Gao, X., & Zhang, Z. (2019). Thermal properties enhancement and application of a novel sodium acetate trihydrate-formamide/expanded graphite shape-stabilized composite phase change material for electric radiant floor heating. *Applied Thermal Engineering, 150*, 1177-1185. doi:https://doi.org/10.1016/j.applthermaleng.2019.01.069

Herbinger, F., & Groulx, D. (2022). Experimental Comparative Analysis of Finned-Tube PCM-Heat Exchangers' Performance. *Applied Thermal Engineering*, 118532. doi:https://doi.org/10.1016/j.applthermaleng.2022.118532

Li, Y., Kumar, N., Hirschey, J., Akamo, D. O., Li, K., Tugba, T., Goswami, M., Orlando, R., LaClair, T. J., Graham, S., & Gluesenkamp, K. R. (2022). Stable salt hydrate-based thermal energy storage materials. *Composites Part B: Engineering, 233*, 109621. doi:https://doi.org/10.1016/j.compositesb.2022.109621

Mao, J., Hou, P., Liu, R., Chen, F., & Dong, X. (2017). Preparation and thermal properties of SAT-CMC-DSP/EG composite as phase change material. *Applied Thermal Engineering, 119*, 585-592. doi:https://doi.org/10.1016/j.applthermaleng.2017.03.097

Pakalka, S., Valančius, K., & Streckienė, G. (2020). Experimental comparison of the operation of PCM-based copper heat exchangers with different configurations. *Applied Thermal Engineering, 172*, 115138. doi:https://doi.org/10.1016/j.applthermaleng.2020.115138

Ruben, H. W., Templeton, D. H., Rosenstein, R. D., & Olovsson, I. (1961). Crystal Structure and Entropy of Sodium Sulfate Decahydrate. *Journal of the American Chemical Society, 83*(4), 820-824. doi:10.1021/ja01465a019

Telkes, M. (1952). Nucleation of Supersaturated Inorganic Salt Solutions. *Industrial & Engineering Chemistry, 44*(6), 1308-1310. doi:10.1021/ie50510a036

Ye, R., Lin, W., Yuan, K., Fang, X., & Zhang, Z. (2017). Experimental and numerical investigations on the thermal performance of building plane containing CaCl2·6H2O/expanded graphite composite phase change material. *Applied Energy, 193*, 325-335. doi:https://doi.org/10.1016/j.apenergy.2017.02.049

ACKNOWLEDGEMENT

This work was sponsored by the U. S. Department of Energy's Building Technologies Office under Contract No. DE-AC05-00OR22725 with UT-Battelle, LLC. The authors would like to acknowledge Mr. Sven Mumme, Technology Manager – Building Envelope, U.S. Department of Energy Building Technologies Office.